Preprint
UCRL-JC-141875

Astrometry with the MACHO Data Archive

A.J. Drake, C. Alcock, R.A. Allsman, D.R. Alves, T.S. Axelrod, A.C. Becker, D.P. Bennett, K.H. Cook, K.C. Freeman, M. Geha, K. Griest, M.J. Lehner, S.L. Marshall, D. Minniti, C.A. Nelson, B.A. Peterson, P. Popowski, M.R. Pratt, P.J. Quinn, C.W. Stubbs, W. Sutherland, T. Vandehei, and D.L. Welch

This article was submitted to
197th Meeting American Astronomical Society, San Diego, CA,
January 08 – 11, 2001

U.S. Department of Energy

Lawrence
Livermore
National
Laboratory

October 15, 2000

This work was performed under the auspices of the United States Department of Energy by the University of California, Lawrence Livermore National Laboratory under contract No. W-7405-Eng-48.

Astrometry with the MACHO Data Archive

A.J. Drake[1], C. Alcock[2,1], R.A. Allsman[3], D.R. Alves[4], T.S. Axelrod[5], A.C. Becker[6], D.P. Bennett[7,1], K.H. Cook[1], K.C. Freeman[5], M. Geha[8,1], K. Griest[9,1], M.J. Lehner[2], S.L. Marshall[1], D. Minniti[10,1], C.A. Nelson[1], B.A. Peterson[5], P. Popowski[1], M.R. Pratt[11], P.J. Quinn[12], C.W. Stubbs[13,5], W. Sutherland[14]T. Vandehei[9] AND D.L. Welch[15]

(The MACHO Collaboration)

ABSTRACT

We present the preliminary results of our astrometric study of stellar motions along the lines of sight of the Magellanic Clouds and the Galactic bulge. We find that we are able to select stars with proper motions as small as 0.03″/yr from five years of PSF photometry due to the characteristic nature of the shapes the light curves of HPM stars. This shape arises from the proper motion of the object relative to the initial fixed centroid location where all photometry of the object is performed. By selecting such light curves and performing astrometry on candidate HPM stars we have discovered 154 new high proper motion (HPM) stars in $50^{\Box o}$ from amongst the $\sim$ 55 million of stars observed by the MACHO project in these fields. These objects have proper motions as high as 0.5″/yr, luminosties ranging from $V \sim 13$ to $V \sim 19$, and $V - R$ colours between 0.3 and 1.45.

[1]Lawrence Livermore National Laboratory, Livermore, CA 94550

[2]Department of Physics and Astronomy, University of Pennsylvania, PA 19104

[3]Supercomputing Facility, Australian National University, Canberra, ACT 0200, Australia

[4]Space Telescope Science Institute, 3700 San Martin Dr, Baltimore, MD 21218

[5]Research School of Astronomy and Astrophysics, Weston Creek, Canberra, ACT 2611, Australia

[6]Bell Laboratories, Lucent Technologies, 600 Mountain Avenue, Murray Hill, NJ 07974

[7]Department of Physics, University of Notre Dame, Notre Dame, IN 46556

[8]Department of Astronomy and Astrophysics, University of California, Santa Cruz, CA 95064

[9]Department of Physics, University of California, San Diego, CA 92093

[10]Departmento de Astronomia, P. Universidad Católica, Casilla 104, Santiago 22, Chile

[11]Center for Space Research, MIT, Cambridge, MA 02139

[12]European Southern Observatory, Karl Schwarzchild Str. 2, D-85748 Gärching bei München, Germany

[13]Department of Physics, University of Oxford, Oxford OX1 3RH, UK

[14]Department of Astronomy and Physics, University of Washington, Seattle, WA 98195

[15]Department of Physics and Astronomy, McMaster University, Hamilton, ON L8S 4M1, Canada

1. Introduction

The MACHO project observed stars in the Magellanic clouds and Galactic bulge in the period between July 21 1992 and January 3 2000 in an effort to detect gravitational microlensing events. Throughout the lifetime of the project photometry was carried out using a modified version of the DoPhot PSF fitting package called SoDoPhot. This package was designed to perform photometry by using the centroid coordinates of stars found in an initial good seeing template observation. These stars were followed up in subsequent observations even when the seeing was poor by simply transforming the template centroid coordinates to those in the new observation.

In most cases the template observation was one of the first images taken of a field. Since the centroid locations are fixed within a field in an initial observation, one naturally expects that an individual star moving relative to most stars in the field will diverge from the centroid location where photometry is performed. This motion relative to the centroid location causes the amount of flux encompassed by the PSF to decrease as the distance between the stars location and the photometry centroid increases. With this in mind the characteristic shape of the light curve for a high proper motion (HPM) star is seen as a decreasing baseline flux with time. As the seeing of each observation varies, superimposed on this decreasing baseline is an increasing a scatter component dependent on seeing and PSF shape. In Figure 1 we present the MACHO light curve of a HPM star discovered within our analysis of light curves. Notice how the seeing strongly effects the measured flux. Tihs is because less flux is contained within the measured PSF the better the seeing is at a given offset.

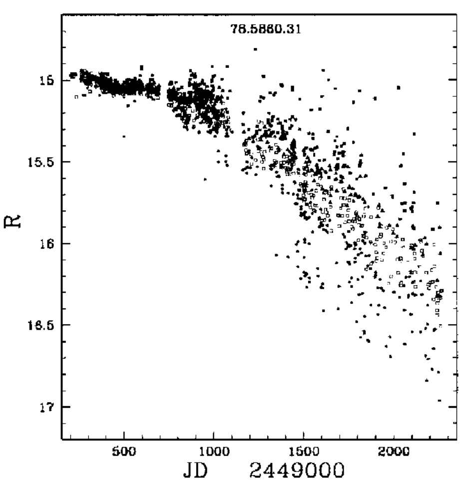

Fig. 1.— An example of the R-band light curve of a LMC candidate high proper motion star (Macho object ID 78.5860.31). The Magenta filled squares are data points with seeing > 5.5 pixels (1 pixel = 0.63″), filled blue triangles are points with seeing between 4.5 and 5.5 pixels, open red squares are points with seeing between 3.5 and 4.5 pixels, green filled pentagons are points with seeing <3.5 pixels.

2. Observations

The MACHO image database contains over 90000 observations of the Galactic bulge and Magellanic Clouds. Each observation consists of 2, 4K $\times$ 4K mosaic images (one in R and one in B) covering an area of $43' \times 43'$ on the sky.

Observations of the Magellanic clouds were taken year round whereas Galactic bulge observations were only taken between March and October each year when the bulge is observable. At the time of this analysis only the first 5 years of photometry have been fully reduced (We expect the remain data to be available within 6 months). The full LMC data set consists of 82 fields each with 5 minute exposure times. However, at present only 30 of these fields have been fully processed corresponding to 11.9 million stars. The SMC data consists of 10 minute exposures in 6 fields with 2.2 million stars. For the Galactic bulge 82 fields have been fully reduced with $\sim$ 40 million stars, here the exposure time was 2.5 mins. For the HPM stars we performed astrometry using observations spanning the full 7.4 years of images.

3. Candidate Selection

To select candidate HPM stars from the photometry we first made a few assumptions about the effect of the motion of the objects centroid relative to the photometry centroid. The amount of flux within the centroid should decrease as the objects centroid diverge from the photometry centroid location. Thus, this decrease in flux should be continuous with increasing time. Hence, on average no positive excursions should be observed. The scatter in the photometry due to seeing should increase with time as the separation between the centroids is increased.

Astrometry was performed on all the candidates which passed the initial photometry selection process. Proper motion offsets were determined by selecting an initial and a final good seeing, low airmass observations of a field. Bright stars within the field were matched between images and are used as reference points for the transformation between images. The two observations used were typically separated by 6.5 years, allowing us to obtain a good S/N for the observed candidates. All candidates HPM stars with 6 sigma centroid offsets were selected as significant objects and were visually inspected to remove any remaining spurious detections due image artifacts such as saturated stars and bad pixels.

We expect that among our initial selection of reference stars there was a $15 - 20\%$ contamination due to foreground stars with higher proper motions, Terndrup (1988, AJ, 96, 884) & Rich (1988, AJ, 95, 828). To remove this bias we applied a 2.3 sigma clipping on references stars while determining the transformation between the initial and images. This should have removed most foreground reference stars with significant proper motions which were not the primary candidate. For the Galactic bulge the remaining stars have a negligible proper motion ($\bar{\mu}_l = 0.''1$ cent^{-1}, $\bar{\mu}_b = 0.''0$ cent^{-1}, Spaenhauer 1992, AJ, 103, 297). For the LMC and SMC measured proper motions are also very small $\sim 1.5 mas/yr$, Drake et al. (2001, in prep.) and Jones et al. (1994, AJ, 107, 1333).

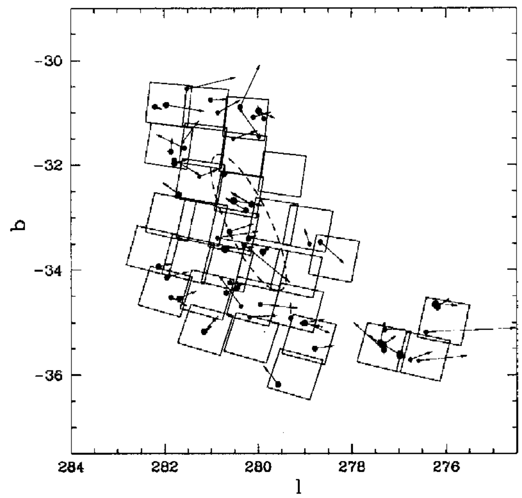

Fig. 2.— The distribution of high proper motion stars detected towards the LMC. The sizes of the dots represents the relative V-band magnitude of the object. The direction and magnitude of the motion vector of each object is shown multiplied by a factor of 2.5×10^4. The blue boxes show the borders of each surveyed field. The dotted line shows the outline of the LMC bar.

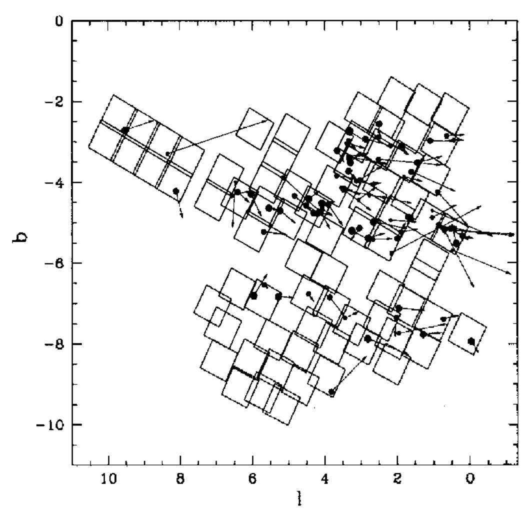

Fig. 3.— The distribution of high proper motion stars detected towards the Galactic bulge. The sizes of the dots represents the relative V-band magnitude of the object. The direction and magnitude of the motion vector of each object is shown multiplied by a factor of 2.5×10^4. The blue boxes show the borders of surveyed fields.

4. Results

In our survey we discovered 154 objects with a significant proper motions selected at a 6σ. The average sigma for these measurements was $0.04''$ (6mas/yr) corresponding to selection level of ~0.25 pixels over the baseline of the experiment. In Figures 2 and 3 we present the locations of the HPM stars detected, along with their directions of motion, for the LMC and Galactic bulge respectively. Notice that the density of HPM objects towards the Galactic bulge is highly inhomogeneous. This is mainly due to the fact that the sampling frequency of high latitude fields is much lower than those close to the Galactic center. This makes it more difficult to detect HPM stars from the photometry. However, there are some regions where there is an over abundance of objects for no apparent reason, for instance near $l = 0.5$, $b = -5$.

In Figure 4 we present images of one of the HPM stars we discovered. In Figure 5 we plot the reduced proper motions of the set of detected objects verses $V - R$. This figure suggests that most of the objects are common main sequence stars.

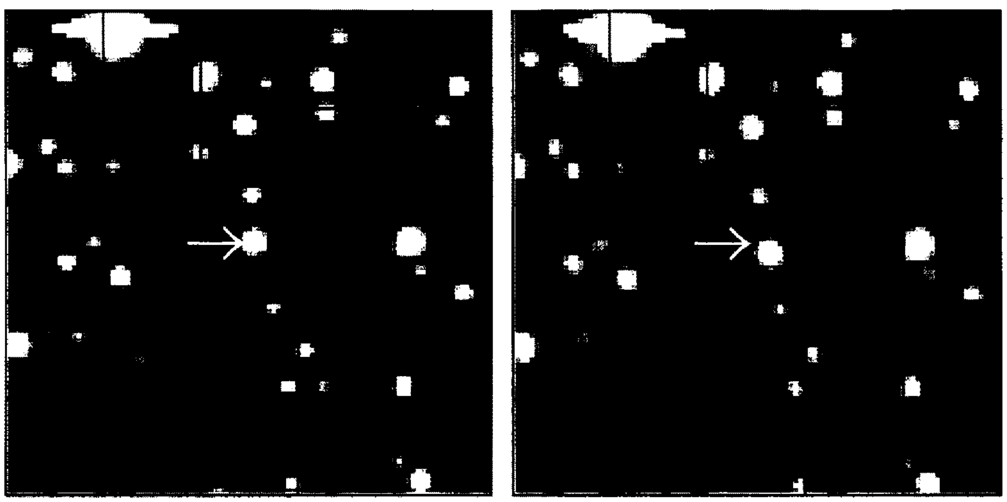

Fig. 4.— Two images of one of the HPM objects (Macho ID 306.36930.78) discovered in this analysis. The proper motion is $0.4''/yr$ and the images are $1' \times 1'$ separated by 4.3 years.

In the survey our HPM object selection is limited to proper motions greater than $\sim 2''/yr$ because light curves of such stars would fall away quickly then remain flat. This case fails our requirement that the flux level falls continously. We note that very few objects fall into this category so there may be no such stars within our fields. HPM stars which are also variables would not be detected with our method. More accurate astrometry could be derived for the objects using a fraction of the number of the observations in each field, rather than just to observations, but this is beyond the scale of our present work.

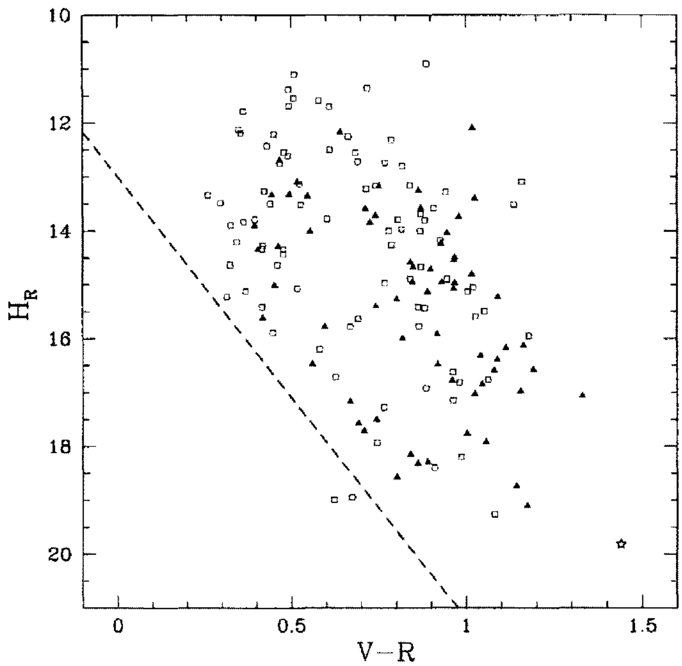

Fig. 5.— Reduced proper motion $H_R = 5 + R + 5\log\mu$ versus colour index $V - R$ diagram of all detected high-proper motion stars. Filled triangles HPM objects towards the Galactic bulge, Open boxes HPM stars towards the LMC, Red star HPM star towards the SMC. Objects lying to the left of the dashed line are candidate White Dwarfs.

4.1. Parallaxes

While selecting HPM stars we discovered a number of good candidates had pronounced oscillations superimposed on the light curve expected for a HPM object. In Figure 5 we present the R and B band light curves of one of these objects. To determine whether this was due to parallax rather than the blending or differential refraction effects we performed astrometry on $\sim$ 300 images spanning the data set. We fitted the astrometry measurements and discovered that the oscillation was not dependent on the seeing or airmass and thus was not due to blending or differential refraction. The parallax measured for this object corresponds to a distance of $\sim$60pc.

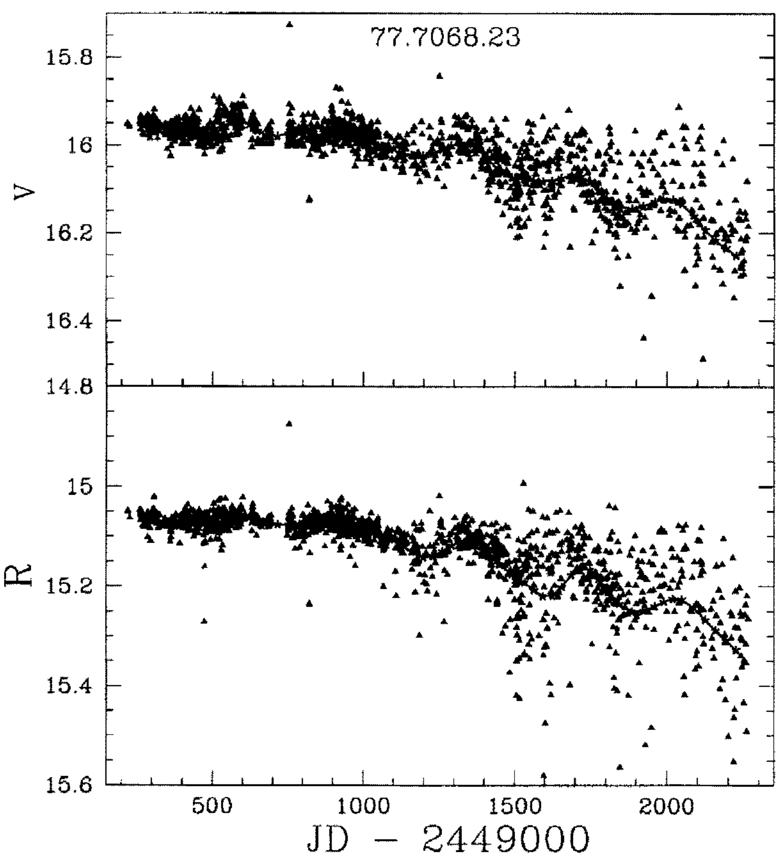

Fig. 6.— The light curve of a high proper motion star exhibiting yearly oscillations in flux due to parallax (Macho ID 77.7068.23). Over-plotted in black is the spline smoothed average magnitude of the data points, clearly showing the presence of oscillation.